JB
Journals.ASM.org

Differential Transcriptional Regulation of *Aggregatibacter actinomycetemcomitans lsrACDBFG* and *lsrRK* Operons by Integration Host Factor Protein

Ascención Torres-Escobar, María Dolores Juárez-Rodríguez, Donald R. Demuth

Research Group in Oral Health and Systemic Disease, University of Louisville School of Dentistry, Louisville, Kentucky, USA

We previously showed that the *Aggregatibacter actinomycetemcomitans lsrACDBFG* and *lsrRK* operons are regulated by LsrR and cyclic AMP receptor protein (CRP) and that proper regulation of the *lsr* locus is required for optimal biofilm growth by *A. actinomycetemcomitans*. Here, we identified sequences that reside immediately upstream from both the *lsrA* and *lsrR* start codons that closely resemble the consensus recognition sequence of *Escherichia coli* integration host factor (IHF) protein. *A. actinomycetemcomitans* IHFα and IHFβ were expressed and purified as hexahistidine fusion proteins, and using electrophoretic mobility shift assays (EMSAs), the IHFα-IHFβ protein complex was shown to bind to probes containing the putative IHF recognition sequences. In addition, single-copy chromosomal insertions of *lsrR* promoter-*lacZ* and *lsrA* promoter-*lacZ* transcriptional fusions in wild-type *A. actinomycetemcomitans* and Δ*ihfA* and Δ*ihfB* mutant strains showed that IHF differentially regulates the *lsr* locus and functions as a negative regulator of *lsrRK* and a positive regulator of *lsrACDBFG*. Deletion of *ihfA* or *ihfB* also reduced biofilm formation and altered biofilm architecture relative to the wild-type strain, and these phenotypes were partially complemented by a plasmid-borne copy of *ihfA* or *ihfB*. Finally, using 5′ rapid amplification of cDNA ends (RACE), two transcriptional start sites (TSSs) and two putative promoters were identified for *lsrRK* and three TSSs and putative promoters were identified for *lsrACDBFG*. The function of the two *lsrRK* promoters and the positive regulatory role of IHF in regulating *lsrACDBFG* expression were confirmed with a series of *lacZ* transcriptional fusion constructs. Together, our results highlight the complex transcriptional regulation of the *lsrACDBFG* and *lsrRK* operons and suggest that multiple promoters and the architecture of the *lsrACDBFG-lsrRK* intergenic region may control the expression of these operons.

The dental biofilm is a complex and dynamic microbial community that comprises up to 700 different species of bacteria (1, 2, 58, 60). This biofilm is the prime etiological agent of three common oral diseases in humans, dental caries, gingivitis, and periodontal disease (3–5, 59). The progression of these diseases is associated with major shifts in microbial populations in the oral biofilm, and diseased sites often exhibit increased populations of pathogenic species relative to healthy sites in the oral cavity (3, 4, 6). The stimuli that contribute to these populational shifts have not been well characterized, but the oral cavity is subject to continual environmental flux, including changes in pH, temperature, osmolarity, and nutrient supply. Oral bacteria rapidly detect and respond to these environmental fluctuations, allowing them to successfully coexist and thrive in the oral cavity (4, 7, 8). Both intra- and interspecies communication is known to occur among oral bacteria, and it is likely that these signaling processes enable the organisms to coordinate their behavior and function by regulating gene expression as a community. One mechanism of communication, termed "quorum sensing," is a cell density-dependent response (9–12), which in Gram-negative bacteria is mediated by the production, release, and detection of soluble signal molecules called "autoinducers."

Aggregatibacter actinomycetemcomitans is a Gram-negative organism that is associated with aggressive forms of periodontitis and other systemic infections (13–16). This organism expresses LuxS and secretes autoinducer 2 (AI-2), and AI-2-dependent quorum sensing has been shown to regulate the expression of virulence factors, iron acquisition systems, and biofilm formation (17–20). The complex regulatory network involved in *A. actinomycetemcomitans* biofilm growth and the role of quorum sensing in this process have begun to be explored in recent years. *A. actinomycetemcomitans* expresses two periplasmic proteins, LsrB and RbsB, that function as receptors for AI-2 (21, 22), and inactivation of either or both of the genes encoding these proteins results in reduced biofilm growth and virulence (18, 20, 21). Like *Escherichia coli* and *Salmonella*, *A. actinomycetemcomitans* LsrB is encoded by an operon consisting of *lsrACDBFG* (the *Salmonella enterica* serovar Typhimurium operon also contains an additional gene designated *lsrE*), where the *lsrACD* genes encode the AI-2 transporter, *lsrF* encodes an aldolase-like protein that cleaves AI-2 (23), and *lsrG* codes for an isomerase of phospho-AI-2 (24). Upstream of and divergently transcribed from the *lsrACDBFG* operon resides *lsrRK*, encoding a repressor of *lsrACDBFG* (LsrR) and an AI-2 kinase (LsrK), which in *E. coli* regulate the expression of *lsrACDBFG* operon in an AI-2-dependent manner (25, 26). In *E. coli* and *S.* Typhimurium, AI-2 is internalized and phosphorylated at high density by LsrK, and AI-2-PO_4 binds to LsrR, resulting in derepression of *lsrACDBFG*. The structure of both operons is conserved in *A. actinomycetemcomitans*, but in contrast to what

Received 2 January 2014 **Accepted** 7 February 2014
Published ahead of print 14 February 2014
Address correspondence to Donald R. Demuth, drdemu01@louisville.edu.
A.T.-E. and M.D.J.-R. contributed equally to this article.
Supplemental material for this article may be found at http://dx.doi.org/10.1128/JB.00006-14.

doi:10.1128/JB.00006-14

occurs in *E. coli*, deletion of *lsrK* had no effect on the transcriptional activity of the *A. actinomycetemcomitans lsrA* or *lsrR* promoters (27). However, deletion of *lsrR*, *lsrRK*, or the gene encoding the cyclic AMP (cAMP) receptor protein (CRP) results in a significant reduction of biofilm formation by *A. actinomycetemcomitans* (27). Thus, the proper regulation of the *lsr* locus has a significant impact on the ability of *A. actinomycetemcomitans* to thrive in biofilms.

The integration host factor (IHF) is a DNA-binding and -bending protein that consists of two subunits, HimA (IHFα) and HimD (IHFβ), which show 30% identity in their amino acids in *E. coli*. IHF recognizes and binds to the asymmetric consensus sequence YAANNNNTTGATW, where Y = T or C, N = any base, and W = A or T (28, 29), which usually is found in A/T-rich regions (30). The surrounding regions flanking the IHF consensus site are also important in the IHF binding (31). IHF was originally discovered as being essential for the integration of the bacteriophage λ DNA into the chromosome (32). However, it is now known to play a role in bacterial chromatin organization, recombination, DNA replication, and transcriptional regulation in Gram-negative bacteria, including the regulation of genetic loci associated with virulence in many pathogenic bacteria. IHF has a critical role in the coparticipation with RpoS for the transcriptional activation of genes required for the transition from exponential growth to the stationary phase, and in *Salmonella*, IHF coordinates the regulation of the major virulence gene clusters. Specifically, IHF has a positive regulatory role in the expression of the pathogenicity island 1 (SP-1) in early and late exponential phases of growth, while at the onset of the stationary phase, IHF inhibits the expression of the genes encoding the type III secretion system (TTSS) and has a positive effect on the expression of the genes coding for secreted effector proteins (33). IHF also has a positive role in the transcriptional control of the *che* genes that encode the chemotaxis proteins and genes coding for the flagellum in *Salmonella* (33), *E. coli* K-12 (34), and *Caulobacter* (35). IHF contributes to flagellin protein phase variation in *Salmonella* (33, 36, 37), and in *E. coli*, IHF participates in the control of phase variation of type 1 fimbria (38). Furthermore, the foundation of the biofilm structure is the extracellular polymeric substance (EPS) that acts as a barrier to protect the bacteria in the biofilm community from host defenses and antibiotics. Extracellular IHF appears to play a role in the integrity of the EPS matrix that contains extracellular DNA, and treatment with IHF antibodies rapidly disrupts the biofilm EPS formed by several human pathogens *in vitro* (39–41).

In this report, we show that the intergenic region (IGR) separating the *A. actinomycetemcomitans lsrACDBFG* and *lsrRK* operons contains two motifs that resemble the consensus IHF binding site and that both interact with purified IHFα-IHFβ complex. We also show that IHF differentially regulates the *lsrACDBFG* and *lsrRK* operons, and deletion of either *ihfA* or *ihfB* reduces biofilm growth by *A. actinomycetemcomitans*. These results highlight the complex transcriptional regulation of the *lsrACDBFG* and *lsrRK* operons and suggest that the architecture of the *lsrACDBFG-lsrRK* intergenic region may contribute to the regulation of these operons.

MATERIALS AND METHODS

Bacterial strains, plasmids, and media. The bacterial strains and plasmids used in this study are listed in Table S1 in the supplemental material. Luria-Bertani (LB) broth, LB agar (LB broth plus 1.5% agar), TYE broth (1% tryptone, 0.5% yeast extract), brain heart infusion (BHI) broth, and BHI agar (all from Difco) were routinely used for the propagation and plating of bacteria. *Aggregatibacter actinomycetemcomitans* (afimbriated, smooth-colony morphotype strain 652) was grown at 37°C under microaerophilic conditions in a candle jar and was also used for biofilm experiments (see below). When required, the medium was supplemented with 25 μg/ml kanamycin (Km), 12.5 μg/ml tetracycline (Tc), 50 μg/ml spectinomycin (Sp), or 100 μg/ml ampicillin (Amp).

DNA procedures. DNA manipulations were carried out as described previously (42). Transformation of *E. coli* and *A. actinomycetemcomitans* was done by electroporation (Bio-Rad, Hercules, CA). Transformants containing plasmids were selected on LB agar plates supplemented with the appropriate antibiotics. Plasmid DNA was isolated using the QIAprep Spin miniprep kit (Qiagen, Valencia, CA). Restriction enzymes were used as recommended by the manufacturer (New England BioLabs, Ipswich, MA). All primers used in this study (Integrated DNA Technology, Coralville, IA) are shown in Table S2 in the supplemental material, and those flanked with restriction enzyme sites are underlined in the primer sequences. Primer sequences were designed based on the genome information of *A. actinomycetemcomitans* strain D11S-1 available from the Pathosystems Resource Integration Center (http://patricbrc.vbi.vt.edu). All constructs were verified by DNA sequencing (University of Louisville Core Sequencing Facilities).

Identification of the *lsrR* and *lsrA* transcriptional start sites. The transcriptional start sites of *lsrR* and *lsrA* were determined using a Gene Racer kit (Invitrogen, Grand Island, NY). *A. actinomycetemcomitans* 652 was grown in LB to the late exponential phase (optical density at 600 nm [OD_{600}] of 0.4). This culture was treated with Qiagen RNAprotect bacterial reagent, and total RNA was extracted using the RNeasy lipid tissue minikit (Qiagen, Valencia, CA) as specified by the manufacturer. RNA was treated with RNase-free DNase I (New England BioLabs, Ipswich, MA) to eliminate contaminating DNA. RNA was quantified by spectrophotometry using a Nanodrop ND-1000 (Thermo Fisher Scientific, Pittsburgh, PA). A 44-base 5′ RNA adaptor oligonucleotide was ligated to the 5′ ends of the total RNA (5 μg) using T4 RNA ligase. Reverse transcription (RT) was performed with avian myeloblastosis virus (AMV) reverse transcriptase and random hexamers that were included in the Gene Racer kit. PCR was performed using the Gene Racer 5′ primer and the *lsrA*- and *lsrR*-specific primers ATE-210 and ATE-208, respectively. The PCR products were subsequently cloned into a pCR4-TOPO vector and transformed into *E. coli* TOP10 (Invitrogen). Thirty-five positive independent clones were sequenced for the *lsrR* promoter, and 28 clones were analyzed for the *lsrACDBFG* promoter.

Construction of *lsrR* and *lsrA* promoter-*lacZ* fusion plasmids. Various fragments containing portions or the entire intergenic region between *lsrACDBFG* and *lsrRK* region were amplified by PCR as follows using *A. actinomycetemcomitans* 652 genomic DNA as a template. The typical amplification profile used was 94°C for 2 min for 1 cycle and then 94°C for 30s, 60°C for 1 min, and 72°C for 2 min for 25 cycles. For the *lsrR* promoter fusion constructs pATE69, pATE70, and pATE100, portions of the intergenic region were amplified using the primer sets ATE-172F and ATE-6R, ATE-173F and ATE-6R, and ATE-242F and ATE-6R, respectively (see Table S2 in the supplemental material). The 193-, 143-, and 414-bp PCR products were then digested with KpnI-BamHI, and each was cloned into KpnI-BamH-digested pJT3 (43) to create pATE69, pATE70, and pATE100, respectively. A similar approach was used to construct the *lsrA* promoter fusion plasmids pATE73, pATE74, and pATE75. The primer sets used to amplify the appropriate promoter fragment for these constructs were ATE-165F and ATE-7R, ATE-166F and ATE-7R, and ATE-167F and ATE-7R, respectively.

Construction of pATE92 and pATE93 plasmids. The promoter region and structural *ihfA* gene were amplified from *A. actinomycetemcomitans* genomic DNA using primer sets ATE-216F and ATE-218R, and the resulting 813-bp fragment was digested with BamHI-XbaI and cloned

into BamHI-XbaI-digested pJT7 (A. Torres-Escobar, M. D. Juarez-Rodriguez, and D. R. Demuth, submitted for publication) (see Table S2 in the supplemental material) to create pATE92. Similarly, the promoter region and structural *ihfB* gene were amplified from *A. actinomycetemcomitans* genomic DNA using primer sets ATE-219F and ATE-221R, and the resulting 714-bp product was digested with KpnI-XbaI and cloned into KpnI-XbaI-digested pJT7 (see Table S2) to create pATE93.

Construction of *ihfA* and *ihfB* expression plasmids. The structural *ihfA* and *ihfB* genes were PCR amplified from *A. actinomycetemcomitans* genomic DNA using primer sets ATE-188F and ATE-189R and ATE-190F and ATE-191R, respectively. The 302-bp product containing the *ihfA* gene and the 285-bp product containing the *ihfB* gene were digested with NcoI-ApaI and cloned individually into the NcoI-ApaI-digested pYA3883 (44) expression vector to create pATE76 and pATE77, respectively. However, IHFβ was only moderately expressed from pATE77; thus, a fragment containing the structural *ihfB* flanked by the sequence encoding the AU1 (44) from pATE77 was amplified using the primer set ATE-192F and ATE-193R in order to increase its expression. The resulting 317-bp PCR product was digested with NcoI-XhoI and cloned into NcoI-XhoI-digested pET28A+ vector (Novagen) to obtain pATE80.

Generation of *A. actinomycetemcomitans* markerless deletion mutants. The construction of *A. actinomycetemcomitans* harboring a markerless deletion mutation of the *ihfA* gene was carried out by amplifying the upstream and downstream flanking regions of *ihfA* with primer sets ATE-157F and ATE-134R and ATE-135F and ATE-158R (see Table S2 in the supplemental material). The respective 646-bp and 546-bp PCR products were digested with NheI-XhoI and XhoI-SacI and cloned adjacently (joined by the XhoI restriction site) into NheI-SacI-digested pJT1 suicide vector (43) to create pATE78. A similar approach was used to generate the markerless deletion mutant in *ihfB*. The upstream and downstream flanking regions of *ihfB* were amplified by PCR with primer sets ATE-159F and ATE-142R and ATE-143F and ATE-160R (see Table S2). The respective 652-bp and 1,035-bp PCR products were digested with NheI-XhoI, and XhoI-SacI and cloned adjacently (joined by the XhoI restriction site) into the NheI-SacI-digested pJT1 suicide vector to create pATE79. Each recombinant suicide plasmid (20 μg) was introduced individually into *A. actinomycetemcomitans* by electroporation. Electroporated cells were incubated in 0.5 ml of SOC broth (Super Optimal broth with glucose added for catabolite repression) standing for 5 h at 37°C under microaerophilic conditions (anaerobic jar). Bacterial cells with single recombinant event were selected onto BHI agar containing 50 μg/ml Sp at 37°C under microaerophilic conditions. Ten spectinomycin-resistant (Sp^r) colonies were randomly selected and subcultured daily for 24 h at 37°C for 3 consecutive days, except that the final cultures were grown in the presence of 1 mM IPTG (isopropyl-β-D-thiogalactopyranoside) (IPTG-induced P_{trc}-*sacB*). To select for bacteria that had undergone a second recombination event, the culture was diluted 10-fold, spread onto TYE agar supplemented with 1 mM IPTG and 10% sucrose, and grown at 37°C under microaerophilic conditions. One thousand sucrose-resistant (Suc^r) colonies were replica plated onto TYE agar supplemented with sucrose and onto BHI agar supplemented with spectinomycin. Spectinomycin-sensitive (Sp^s) colonies were selected to perform PCR for the deletion mutation of the target genes, using the primer set ATE-137F and ATE-140R for *ihfA* deletion or ATE-145F and ATE-148R for *ihfB* deletion. Sp^s colonies that were PCR positive were selected for further analysis.

Integration of *lsrR-lacZ* or *lsrA-lacZ* transcriptional fusion in single copy into the *A. actinomycetemcomitans* genome. To integrate a single copy of the *lsrR*-promoter- or *lsrA*-promoter-*lacZ* transcriptional fusions into the chromosome of *A. actinomycetemcomitans* by homologous recombination, the *lsrR-lacZ* (in a 3,000-bp KpnI-XbaI fragment) and *lsrA-lacZ* (in a 3,969-bp KpnI-XbaI fragment) constructs were released from pATE23 and pATE75, respectively, and were subcloned into KpnI-XbaI-digested pJT10 suicide vector (Torres-Escobar et al., submitted) to create pATE94 and pATE95, respectively. Each recombinant suicide plasmid (20 μg) was introduced individually into *A. actinomycetemcomitans* 652 and isogenic Δ*ihfA*, and Δ*ihfB* mutants by electroporation. A similar approach used to generate the markerless deletion mutants described above was employed, but with the selection of Sp^r colonies, to obtain *A. actinomycetemcomitans* with a single copy of the transcriptional fusion inserted in the chromosome by one homologous recombinant event. Ten Sp^r colonies were selected to verify by PCR the single-copy chromosomal insertion of the *lsrR-lacZ* or *lsrA-lacZ* fusion with primer sets ATE-210R and MDJR-123R and MDJR148F and ATE208R and ATE-208R and MDJR-123R and MDJR148F and ATE210R, respectively. The Sp^r colonies that were PCR positive were selected for further analysis.

Growth kinetics. A single colony of *A. actinomycetemcomitans* harboring each recombinant plasmid was independently inoculated into 10 ml of BHI medium supplemented with 25 μg/ml Km and was grown standing for 24 h at 37°C. The next day, the overnight culture (OD_{600} of 0.6) was diluted at a 1:30 ratio to inoculate 10 ml of BHI with 25 μg/ml Km and grown standing at 37°C. For the first 12 h of growth, an aliquot was removed each hour, and culture density was determined by measuring the OD_{600}. Additional aliquots were taken from each culture for analysis at the 24-, 48-, and 72-h time points. β-Galactosidase (β-Gal) activity was also determined for each aliquot as described below.

β-Gal assays. β-Galactosidase (β-Gal) activity was qualitatively assessed on LB agar plates that were supplemented with 50 μg/ml 5-bromo-4-chloro-3-indolyl-β-D-galactopyranoside (X-Gal). Quantitative evaluation of β-Gal activity was carried out using permeabilized cells incubated with *o*-nitrophenyl-β-D-galactopyranoside (ONPG) substrate (Sigma, St. Louis, MO) as previously described by Miller (45). Average values ± standard deviations) for activity units were routinely calculated from three independent assays, each carried out in triplicate.

Expression and purification of IHF protein. *E. coli* LMG194 harboring pATE76 and *E. coli* BL21(DE3) transformed with the pATE80 plasmid were used for the synthesis of the hexahistidine fusion proteins' IHF alpha (IHFα) and beta (IHFβ) subunits, respectively. The expression and detection of the recombinant proteins were performed essentially as described previously by Torres-Escobar et al. (44). Purification was carried out by cobalt-based immobilized metal affinity chromatography under denaturing conditions. Eluted fractions containing the purified IHFα and IHFβ subunits were selected based on sodium dodecyl sulfate-polyacrylamide gel electrophoresis analysis (SDS-PAGE). The IHFα and IHFβ selected pools were mixed in equimolar quantities and dialyzed in a Slyde-A-Lyzer 3K cassette (Pierce) at 4°C against refolding buffer containing 50 mM Tris-HCl (pH 8.5), 4 M urea, 0.5 M L-arginine, 264 mM NaCl, 11 mM KCl, 8 mM $MgCl_2$, 0.1% Triton X-100, and 20% (vol/vol) glycerol for 24 h. Subsequently, samples were dialyzed for 24 h against the buffer described above but containing 2 M urea and then sequentially dialyzed for 12 h each in buffer consisting of 50 mM Tris-HCl (pH 8.5), 100 mM NaCl, 0.1 mM KCl, 4 mM $MgCl_2$, 2 mM $Mg(CH_3COO)_2$, 0.1 mM EDTA, 0.1 mM dithiothreitol (DTT), 50% (vol/vol) glycerol, and 2, 1, or 0.5 M urea. A final dialysis was then carried out for 6 h against the buffer described above without urea. Aliquots of the IHF heterodimer reconstituted from purified subunits IHFα and IHFβ was stored at −70°C. The protein concentration was determined by the Bradford assay, using bovine serum albumin (BSA) as a standard.

EMSA. The DNA fragments used for the nonradioactive electrophoretic mobility shift assay (EMSA) were obtained by PCR using sets of primers described in Table S2 in the supplemental material. A biotin 3′-end labeling kit (Fisher Scientific, Pittsburgh, PA) was used for labeling of DNA fragments according to the manufacturer's instructions. Binding reactions were performed with a total of 50 fmol of each probe mixed with various amounts of the IHF heterodimer reconstituted from purified subunits IHFα and IHFβ (1, 2, and 4 μM) in 20 μl of binding buffer consisting of 10 mM Tris-HCl [pH 7.5], 50 mM KCl, 1 mM dithiothreitol, 1 μg poly(dI-dC), and 100 μg/ml bovine serum albumin (BSA). The reaction mixtures were incubated for 20 min at room temperature. Afterward, 5 μl of gel loading buffer (0.25× Tris-borate-EDTA [TBE], 60%; glycerol, 40%; bromophenol, 0.2% [wt/vol]) was added, and the mixtures were

electrophoresed in a 6% native polyacrylamide gel in 0.5× TBE buffer (45 mM Tris-borate, 1 mM EDTA [pH 8.0]) and immunoblotted. DNA bands were detected using the LightShift chemiluminescent EMSA kit according to the manufacturer's instructions.

Biofilm formation and analysis. *A. actinomycetemcomitans* biofilms were grown in an FC81 polycarbonate flow chamber (Biosurface Technologies Corp., Bozeman, MT) (chamber dimensions are 50.5 mm by 12.7 mm by 2.54 mm) at a flow rate of 10 ml per hour at 25°C, essentially as described by Shao et al. (20). The resulting biofilm was stained with 0.2 mg/ml fluorescein isothiocyanate (FITC) (Sigma-Aldrich) for 1 h in the dark and then washed with phosphate-buffered saline (PBS) for 2 h. Biofilms were visualized using an Olympus Fluoview FV500 confocal scanning laser microscope (Olympus, Pittsburgh, PA) at a magnification of ×600, using an argon laser. Confocal images were captured from 20 randomly chosen frames from each flow chamber, and z-plane scans from 0 to 100 μm at 1-μm intervals were performed above the glass surface for each frame. The images were analyzed using Volocity image analysis software (PerkinElmer, Inc., Waltham, MA) to reconstruct three-dimensional images. Biofilm depth, biofilm biomass, and total surface area of biofilm were determined using the Volocity software package. The values reported are means of data from the different frames obtained. Biofilm assays were repeated independently three times with each strain. Differences among biofilms were determined by one-way analysis of variance (ANOVA) followed by Tukey's multiple-comparison test. Differences with P values of <0.05 were considered significant. Data were analyzed with GraphPad Prism v5 software.

RESULTS

Identification of putative integration host factor binding sites in the *lsrACBFG* and *lsrRK* operon promoters. In our previous work, we identified key promoter elements in a 414-bp sequence that encompasses the intergenic region between the divergent *lsrACBFG* and *lsrRK* operons in *A. actinomycetemcomitans* and showed that the expression of these operons was controlled by both the LsrR repressor and cAMP receptor protein (CRP) (27). We have now identified two additional sequences in the 414-bp intergenic region that closely resemble the *E. coli* consensus recognition sequence of the integration host factor (IHF) protein (YAANNNNTTGATW, where Y = T or C, N = any base, and W = A or T) (29). The first putative IHF binding sequence is located at nucleotides −65 to −77 relative to the *lsrR* start codon. The second sequence comprises nucleotides −66 to −78 relative to the putative *lsrA* start codon (27). These sequences have been designated $IHFs_1$ and $IHFs_2$, respectively (for details, see Fig. 2). Furthermore, examination of the *A. actinomycetemcomitans* genome sequence identified two open reading frames designated D11S_1364 and D11S_1626, which are annotated *ihfA* and *ihfB*, respectively (see Fig. S1A in the supplemental material). These genes encode proteins that exhibit 82% and 78% amino acid sequence similarity with *E. coli* IHFα and IHFβ, respectively (not shown) and 40% sequence identity compared to each other (see Fig. S1B).

IHF interacts with the *lsrACDBFG-lsrRK* intergenic region of *A. actinomycetemcomitans*. To determine if the *A. actinomycetemcomitans* IHF protein interacts with the putative binding sites identified in the *lsrA* and *lsrR* promoters (*lsrA*P and *lsrR*P), *A. actinomycetemcomitans* IHFα and IHFβ were expressed as hexahistidine fusion proteins and purified as described in Materials and Methods. The purified individual subunits and a heterodimer made by incubating equimolar concentrations of the individual subunits are shown in Fig. 1. Using the purified heterodimer preparation, EMSA reactions were performed with a family of DNA fragments that spanned the 414-bp promoter sequence (Fig. 2A).

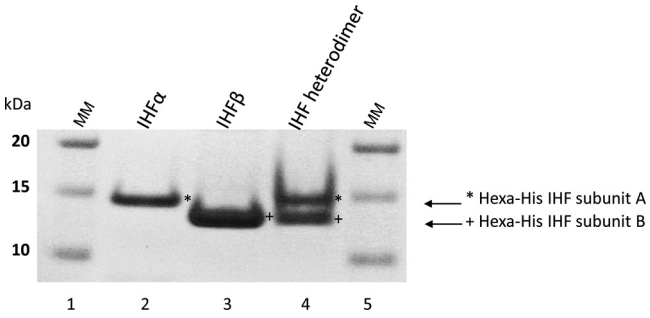

FIG 1 SDS-PAGE analysis of hexahistidine IHF α and β fusion subunits expressed in the cytoplasm of the *E. coli* LMG109 and BL21(DE3) strains. Lane 1, molecular mass marker (MM); lanes 2 and 3, hexahistidine IHFα and IHFβ subunits, respectively, purified by cobalt-based immobilized metal affinity chromatography; lane 4, IHFα and -β subunits from reconstituted IHF heterodimer (at a 1:1 molar ratio) as described in Materials and Methods.

Preliminary experiments showed that the protein and probe concentrations required for optimal formation of DNA-protein complexes were 4 μM and 50 fmol, respectively (data not shown). As shown in Fig. 2B, IHF bound only to probes that contained the putative binding sites described above (i.e., probes III, IV, V, VI, VIII, IX, X, and XI), whereas probes comprising other regions of the IGR or coding sequences of *lsrA* or *lsrR* did not form DNA-IHF complexes (i.e., probes I, II, VII, and XII). Interestingly, upon interaction with $IHFs_2$, the IHF protein produced a single shifted band when incubated with probes III, IV, and VI and two shifted bands with probe V. Similarly, when binding to $IHFs_1$, a single shifted band was detected for probe XI, but multiple shifted bands were observed using probes VIII, IX, and X. There are several possible explanations for this observation: IHF binding may be influenced by sequences flanking the core consensus sequence, IHF binding may be altered when the binding site resides close to the 5′ end of the probe, or alternatively, IHF may induce different DNA-protein conformations in the various probes. IHF binding was not detected using a 200-bp DNA fragment derived from the *Yersinia pseudotuberculosis psaA* gene, which represented a negative control. Together, these results indicate that IHF interacts with both the *lsrRK* and *lsrACDBFG* promoters.

IHF regulates the expression of the *lsrACDBFG* and *lsrRK* operons in *A. actinomycetemcomitans*. Single-copy chromosomal insertions of the *lsrR* promoter-*lacZ* or *lsrA* promoter-*lacZ* transcriptional fusion constructs were introduced into *A. actinomycetemcomitans* 652 (to generate strains 652-TE-23 and 652-TE-75) and its isogenic Δ*ihfA* and Δ*ihfB* mutant strains (producing stains 652-TE78-23, 652-TE78-75, 652-TE79-23, and 652-TE79-75), as described in Materials and Methods. β-Galactosidase (β-Gal) activity expressed by these strains was measured to determine if the IHF protein influences the expression of the *lsrACDBFG* and/or *lsrRK* operon. As shown in Table 1, β-Gal expression directed by the *lsrR* promoter was induced by 4-fold in both the Δ*ihfA* and Δ*ihfB* mutant strains. In contrast, β-Gal expression directed from the *lsrA* promoter decreased by 4- to 6-fold in the Δ*ihfA* or Δ*ihfB* strain. Thus, IHF interacts with each promoter, but the binding of IHF differentially regulates the expression of the *lsrRK* and *lsrACDBFG* operons, reducing the expression of *lsrRK* and inducing *lsrACDBFG*.

Transcription of the *lsrRK* and *lsrACDBFG* operons initiates from multiple sites. 5′ rapid amplification of cDNA ends (5′-

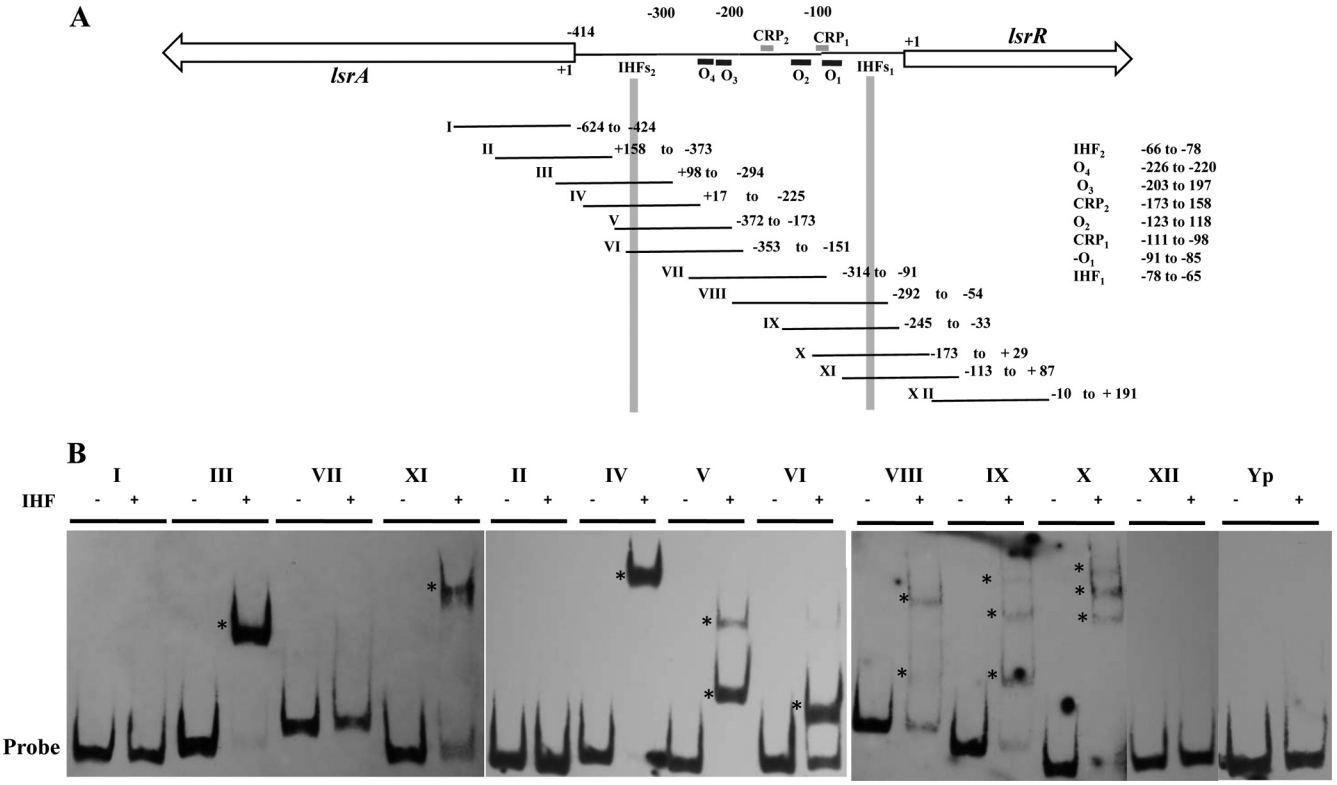

FIG 2 Binding of reconstituted IHF heterodimer to the *lsrA* and *lsrR* promoters. (A) Schematic representation of the *lsrA-lsrR* promoter region showing the putative binding regions for LsrR (black boxes), CRP (gray boxes), and IHF. PCR fragments used for EMSA reactions encompassing the *lsrA* and *lsrR* coding regions and the promoter sequence are numbered from I to XII, and the nucleotides contained by each fragment are indicated to the right. The numbering of the nucleotides comprising the 414-bp promoter sequence is relative to the start codon of *lsrR*. (B). PCR probes were incubated in the presence (+) or absence (−) of 4 μM reconstituted IHF heterodimer for 20 min at room temperature, and DNA-protein complexes (indicated by asterisks) were resolved in 6% polyacrylamide gels. A 200-bp DNA fragment from the *psaA* gene of *Yersinia pseudotuberculosis* (probe Yp) was used as the negative control.

RACE) was employed to map the transcriptional start sites (TSSs) for both the *lsrACDBFG* and *lsrRK* promoters. As shown in Table 2, two TSSs (referred to as TSS_{R1} and TSS_{R2}) were mapped upstream from the *lsrR* start codon. The main start site (TSS_{R1}) mapped to nucleotide −38 and represented 86% of the positive clones that were identified by 5′-RACE. A secondary TSS (TSS_{R2}) mapped to nucleotide −138. In support of these results, putative −10 and −35 elements are present upstream from both TSSs, at nucleotides −41 to −46 and −66 to −71 for TSS_1 and −144 to −149 and −168 to −173 for TSS_2. As shown in Fig. 3, the putative −35 element associated with TSS_1 overlaps the $IHFs_1$ binding site and the putative −35 element for TSS_2 overlaps the CRP_2 binding site that was previously identified (27). These results suggest that two promoters, RP1 and RP2, may drive the expression of *lsrRK*.

Three TSSs (designated TSS_{A1}, TSS_{A2}, and TSS_{A3}) were mapped for the *lsrACDBFG* operon. The main TSS (TSS_{A2}) was located 210 nucleotides upstream from the *lsrA* start codon and represented 60% of the clones that were identified by 5′-RACE. Two secondary TSSs mapped to nucleotides −184 (TSS_{A1}) and −262 (TSS_{A3}) relative to the putative *lsrA* start codon (27), and these sites represented 28% and 11% of the 5′-RACE clones identified, respectively (Table 2). Consistent with these assignments, putative −10 and −35 elements were associated with each TSS, located at nucleotides −191 to −196 and −212 to −217 for TSS_{A1}, −215 to 220 and −238 to 243 for TSS_{A2}, and −268 to 273 and −293 to 298 for TSS_{A3} (Fig. 3). Similar to the results for the *lsrRK* promoter, the

TABLE 1 Differential regulation of the *lsrRK* and *lsrACDBFG* promoters by IHF

Strain	Genotype	β-Galactosidase activity (Miller units)
652-TE-23	Wild type-*lsrR*::*lsrR23-lacZ*	33.3 ± 1.1
652-TE78-23	Δ*ihfA-lsrR*::*lsrR23-lacZ*	123.5 ± 0.9
652-TE79-23	Δ*ihfB-lsrR*::*lsrR23-lacZ*	133.0 ± 3.4
652-TE-75	Wild type-*lsrA*::*lsrA75-lacZ*	96.6 ± 3.7
652-TE78-75	Δ*ihfA-lsrA*::*lsrA75-lacZ*	17.1 ± 0.8
652-TE79-75	Δ*ihfB-lsrA*::*lsrA75-lacZ*	23.8 ± 0.6

TABLE 2 Transcriptional start sites identified by 5′-RACE

TSS	Position (nucleotide)[a]	No. (%) of 5′-RACE clones identified
lsrR		
TSS_1	−38 (A)	30 (86)
TSS_2	−138 (A)	5 (14)
lsrA		
TSS_1	−184 (G)	8 (29)
TSS_2	−210 (A)	17 (60)
TSS_3	−262 (A)	3 (11)

[a] The letter in parentheses indicates the nucleotide determined for that 5′ end.

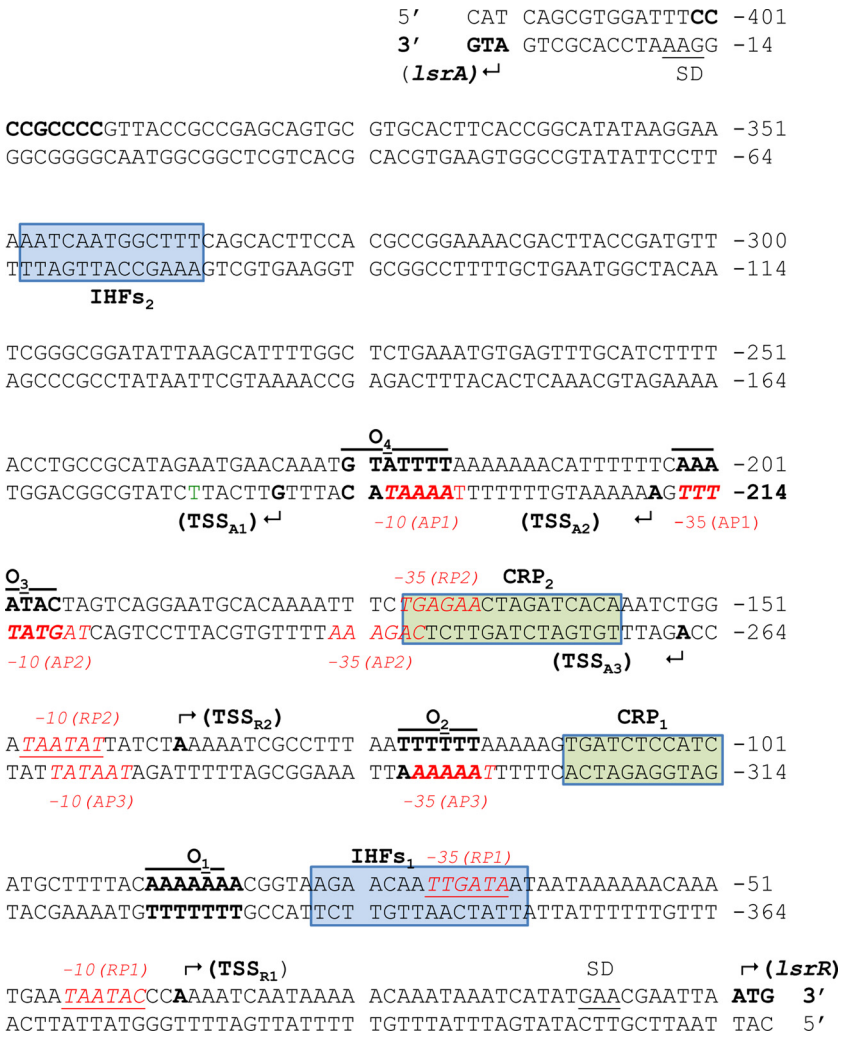

FIG 3 Double-stranded DNA sequence of the 414-bp *lsrA-lsrR* promoter region. The numbers on the top and bottom strands are relative to the *lsrR* and *lsrA* start codons, respectively. Inverted repeat sequences that represent LsrR binding sites are labeled "O_1" to "O_4." Regions that resemble the consensus CRP binding site are shown in green boxes and are labeled "CRP_1" and "CRP_2." Regions that resemble the consensus IHF binding site are shown in blue boxes and are labeled "$IHFs_1$" and "$IHFs_2$." The transcriptional start sites are indicated with bent arrows. For *lsrR*, start sites are labeled "TSS_{RX}"; for *lsrA*, start sites are labeled "TSS_{AX}." Predicted −35 and −10 sequences are shown in shown in red text. Potential Shine-Dalgarno sequences are labeled "SD."

−10 and −35 elements associated with TSS_{A1} overlap the LsrR binding sites O_4 and O_3, which were previously characterized (27). In addition, the −10 element associated with TSS_{A2} overlaps the LsrR binding site, O_3, and its corresponding −35 element overlaps a previously identified CRP_2 binding site. Finally, the −35 element associated with TSS_{A3} overlaps the LsrR binding site O_2. Thus, similar to the *lsrRK* operon, multiple promoters (AP1, AP2, and AP3) may control the expression of *lsrACDBFG*. Overall, these results suggest that several regulatory proteins, including IHF, LsrR, and CRP, interact with multiple overlapping promoters to regulate the expression of the *lsrACDBFG* and *lsrRK* operons in *A. actinomycetemcomitans*.

Functional characterization of the *lsrACDBFG* and *lsrRK* promoters. Our previous results suggested that the *lsrRK* promoter resides within nucleotides −1 to −255 upstream of the *lsrR* start codon (27). As shown in Fig. 4A, there was no significant difference in *lacZ* expression produced from constructs pATE23 and pATE100, confirming that no additional regulatory elements required for expression of *lsrRK* exist between nucleotides −256 and −414. In contrast, our previous results showed that the 255-bp fragment did not promote the expression of *lsrA*, but the entire 414-bp sequence was necessary for expression of *lsrACDBFG* (27). The results presented above now suggest that both the *lsrRK* and *lsrACDBFG* promoter regions contain multiple transcriptional initiation sites, and to demonstrate the function of the putative promoters associated with these TSSs, a series of DNA fragments encompassing portions of the 414-bp IGR were amplified by PCR and cloned individually into the low-copy-number promoterless *lacZ* plasmid pJT3 (Fig. 4). The recombinant plasmids and a control vector without a promoter were introduced into *A. actinomycetemcomitans* by electroporation, and β-galactosidase (β-Gal) activity was determined. As shown in Fig. 4A, a 5-fold reduction in β-Gal expression occurred when nucleotides −1 to −81 upstream from *lsrR* were deleted (see pATE68). This suggests that RP1 is the main promoter driving *lsrRK* expression under the growth conditions tested and is consistent with our

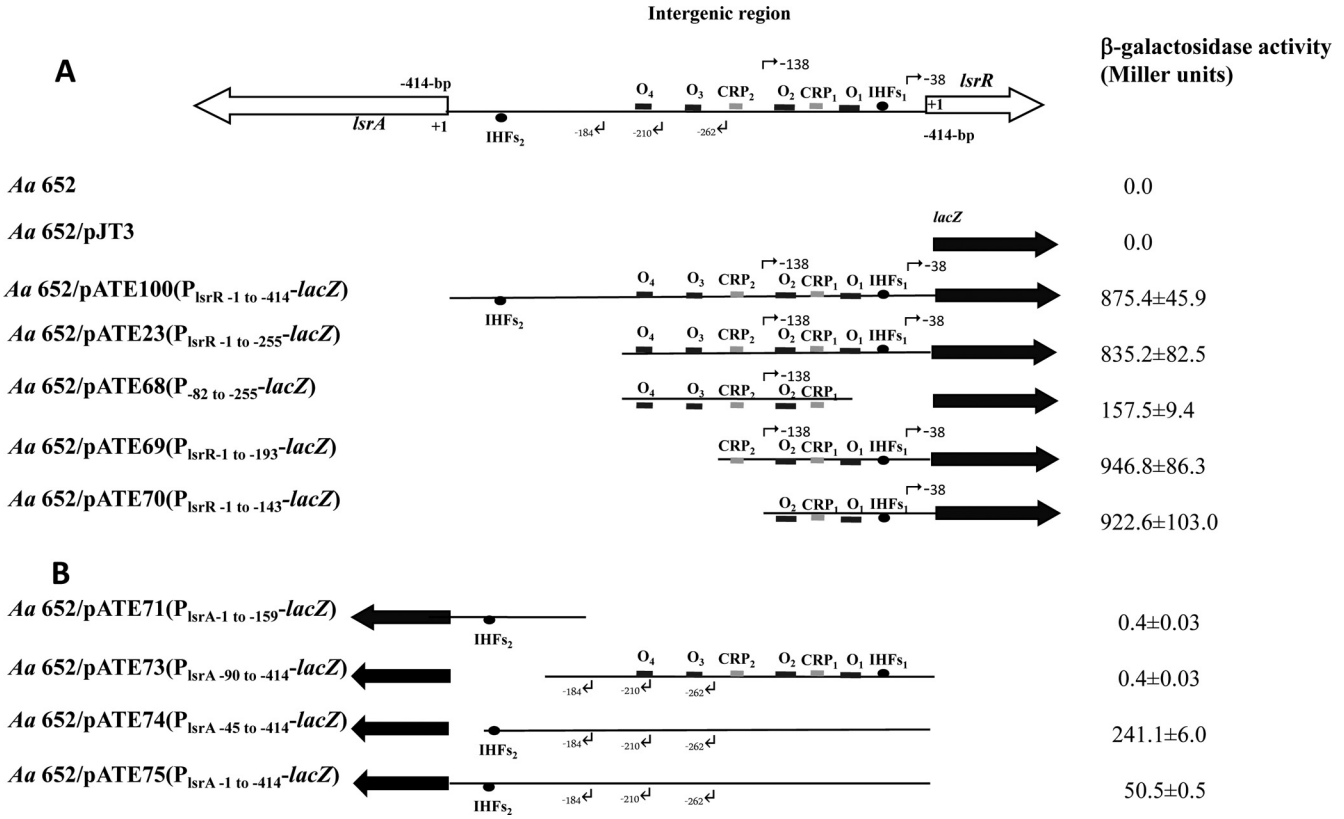

FIG 4 Schematic diagrams of the *lsrR* (A) and *lsrA* (B) transcriptional fusion constructs showing the putative binding regions for LsrR (black boxes labeled "O_1" to "O_4"), CRP (gray boxes), IHF (solid ovals), and transcriptional start sites (bent arrows). Fragments derived from the 414-bp promoter fragment are represented by thin lines, and the *lsrA* and *lsrR* coding sequences are shown by the large open arrows. The numbering of the nucleotides is relative to the *lsrR* start codon in panel A and from the putative *lsrA* start codon in panel B. The *lacZ* gene is indicated by a solid black arrow. β-Galactosidase activity for each construct is expressed as Miller units and was measured in *A. actinomycetemcomitans* (*Aa*) strains transformed individually with each plasmid and grown in BHI medium as described in Materials and Methods. Measurements were made at the mid-exponential phase of growth, and values are means of results from three independent experiments ± standard deviations.

results indicating that TSS_{R1} is the major TSS of the *lsrRK* operon (Table 1). However, even in the absence of RP1, significant β-Gal expression was observed, indicating that RP2 is also functional and contributes to *lsrRK* expression. Deletion of the LsrR binding sites O_3 and O_4 (pATE69 in Fig. 4A) resulted in a modest increase in *lacZ* expression, suggesting that O_1 and O_2 may be the primary sites for the LsrR-mediated repression of *lsrRK* that was previously reported (27).

As shown in Fig. 4B, little *lacZ* expression occurred in the strain containing pATE71, in which the putative promoter elements associated with the three TSSs identified above were deleted. In addition, similar low levels of *lacZ* expression were observed with pATE73, where $IHFs_2$ was deleted but the upstream promoter elements were left intact. This suggests that IHF is a positive regulator of *lsrA* expression, consistent with the results shown in Table 1. This was further confirmed by restoring $IHFs_2$ in construct pATE74, which produced significantly higher levels of *lacZ* expression. Interestingly, *lacZ* expression from pATE74 was approximately 5-fold higher than that observed with pATE75, which contains the entire 414-bp promoter fragment, suggesting that an additional *lsrA* negative regulatory element may exist in the region comprising nucleotides −1 to −44 relative to the putative *lsrA* start codon. At present, it is not known if this putative element functions at the transcriptional or posttranscriptional level.

IHF influences biofilm formation by *A. actinomycetemcomitans*. We previously showed that deletion of *lsrR* or *crp* reduced biofilm growth of *A. actinomycetemcomitans*, suggesting that proper regulation of *lsrACDBFG* and *lsrRK* expression is important for the formation of *A. actinomycetemcomitans* biofilms (27). To determine if deletion of IHF affected biofilm formation, strains 652-TE-78 and 652-TE-79 (Δ*ihfA* and Δ*ihfB*, respectively) were cultured in flow cells, and the resulting biofilms were analyzed by confocal laser scanning microscopy using Volocity software. Representative reconstructed three-dimensional images of the biofilms formed by each strain are shown in Fig. 5, and measurements of biofilm biomass, depth, and surface coverage are presented in Table 3. Deletion of *ihfA* or *ihfB* resulted in a significant decrease in biofilm depth and an increase in total biomass relative to the wild type. Biofilms produced by the mutant strains appeared less structured than the wild type and more closely resembled a confluent layer of cells (and thus a higher total surface coverage) rather than the distinct microcolonies observed with wild-type strain 652. Consistent with this, average biomass per microcolony was significantly increased in the mutant strains since the Volocity software delineated fewer distinct microcolonies (Table 3). Complementation of the Δ*ihfA* and Δ*ihfB* strains with the low-copy-number plasmids pATE92 and pATE93 (copy number of approximately 5 to 10 per cell) containing the promoter and the

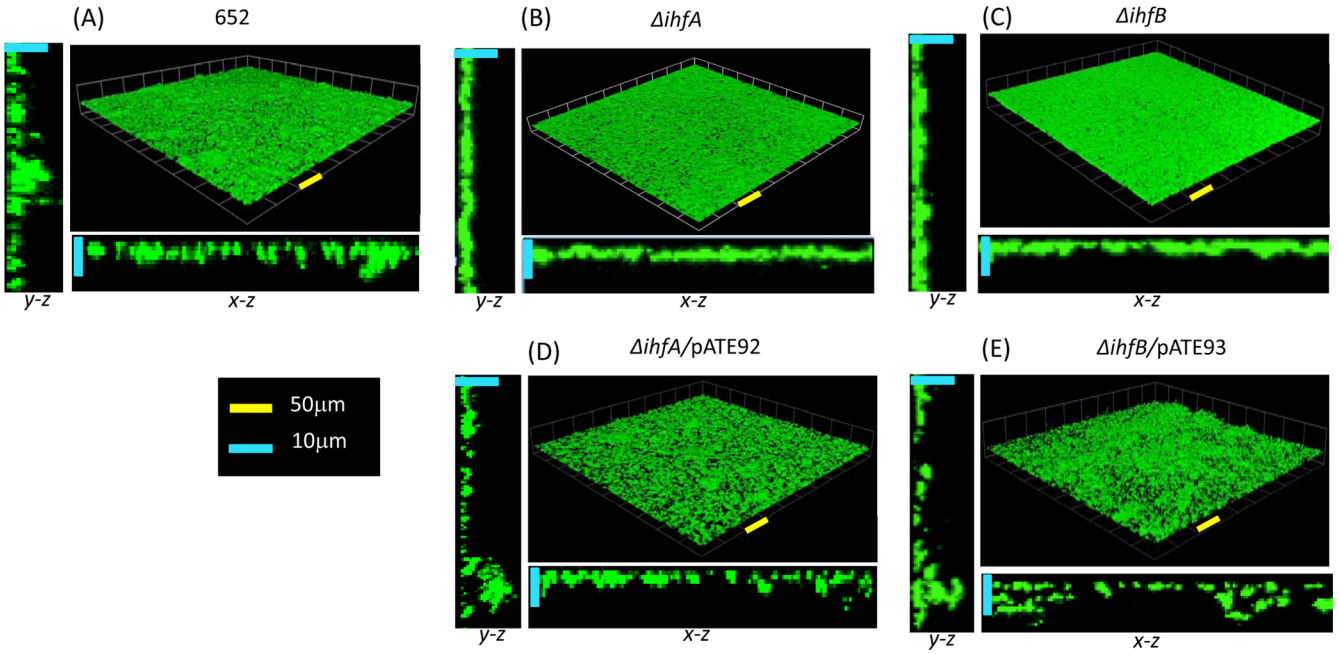

FIG 5 Three-dimensional reconstructions of biofilms formed by wild-type *A. actinomycetemcomitans* 652 (A) and isogenic Δ*ihfA* (B) and Δ*ihfB* (C) mutants. Mutations were complemented by a plasmid-borne copy of *ihfA* or *ihfB* in plasmids pATE92 and pATE93 (D and E), respectively. Biofilms were cultured in open flow cells as described in Materials and Methods and were visualized by confocal laser scanning microscopy. Image stacks were assembled and analyzed using Volocity image analysis software. The yellow and blue scale bars in the *x-y*, *x-z*, and *y-z* sections represent 50 μm and 10 μm, respectively.

structural *ihfA* and *ihfB* genes, respectively, resulted in a biofilm phenotype that was similar to the that of the wild type (Fig. 5D and E). However, total biomass of the complemented cultures was less than that of the parent strain and could be due to the effect of multiple copies of the *ihfA* and *ihfB* genes in these strains. Together, these results suggest that *ihfA* and *ihfB* are required for biofilm formation by *A. actinomycetemcomitans* and may act at least in part through the regulation of the *lsrRK* and *lsrACDBFG* loci.

DISCUSSION

In *E. coli* and *S.* Typhimurium, the products of the divergent *lsrACDBFG-lsrRK* operons are involved in a regulatory network that controls the uptake and processing of autoinducer 2 (AI-2). The structure of both operons is conserved in *A. actinomycetemcomitans*, and recent results from our laboratory showed that the LsrR repressor protein and cyclic AMP receptor protein (CRP) regulate the expression of both the *lsrACDBFG* and *lsrRK* operons in *A. actinomycetemcomitans* (27). As currently annotated, the *A. actinomycetemcomitans* D11S genome indicates that a 255-bp intergenic region resides between *lsrACDBFG* and *lsrRK*, and our present results indicate that all of the regulatory elements required to control the expression of *lsrRK* reside within this sequence. However, the 255-bp fragment did not function as the *lsrA* promoter, but instead, expression of *lsrACDBFG* required an additional 159 nucleotides comprising nucleotides +1 to +158 of the annotated *lsrA* sequence. This led us to speculate that the *lsrA-lsrR* intergenic region might comprise 414 bp and the actual *lsrA* start codon may be the ATG at nucleotides +159 to +161 of the annotated *lsrA* gene (27). Examination of the region from −256 to −414 identified a sequence ($IHFs_2$) that resembled the *E. coli* consensus IHF binding site at nucleotides −66 to −78 upstream from the putative *lsrA* start codon, and EMSA showed that purified IHFα-IHFβ complex bound to probes containing this sequence. IHF functions as a positive regulator of *lsrACDBFG* expression, since deletion of $IHFs_2$ and expression of a single-copy *lsrA* promoter-*lacZ* reporter in the Δ*ihfA* and Δ*ihfB* backgrounds both resulted in a significant reduction in *lacZ* expression. The mechanism of IHF-mediated induction *lsrA* operon expression is cur-

TABLE 3 Analysis of *A. actinomycetemcomitans* biofilms[a]

Strain	Maximal biofilm depth (μm)	Biomass ($\mu m^3 \times 10^3$)		Total surface area ($\mu m^2 \times 10^3$)
		Avg of microcolony	Total	
652	12.19 ± 1.6	4.7 ± 1.5	594.9 ± 47.7	808.1 ± 25.1
Δ*ihfA* mutant	7.59 ± 1.4§	67.6 ± 40†	690.3 ± 58.8†	784.0 ± 19.2
Δ*ihfB* mutant	8.35 ± 1.1*	95.7 ± 70‡	745.9 ± 21.8‡	891.5 ± 75.8§
Δ*ihfA*/pATE92 mutant	14.89 ± 3.8	0.78 ± 0.3	376.6 ± 41.2‡	643.8 ± 30.3‡
Δ*ihfB*/pATE93 mutant	12.11 ± 4.3	0.19 ± 0.05	283.6 ± 43.6‡	515.6 ± 61.9‡

[a] Significance: *, $P < 0.05$; §, $P < 0.01$; †, $P < 0.001$; ‡, $P < 0.0001$.

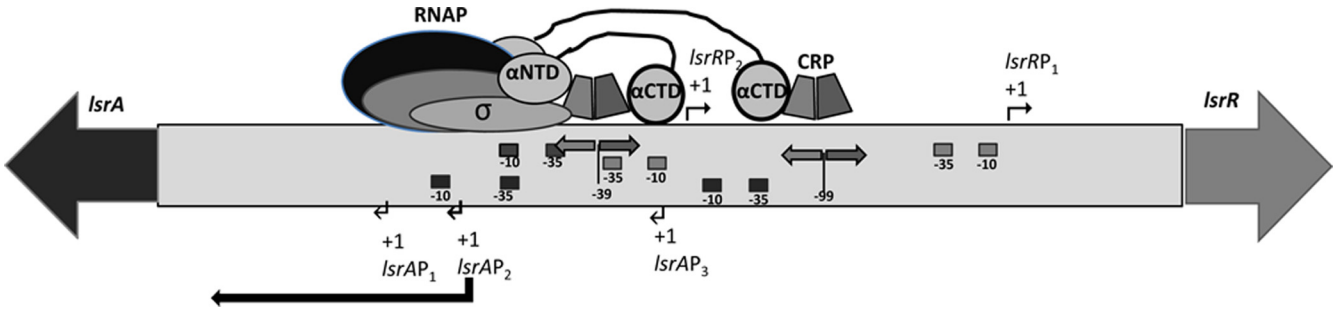

FIG 6 Model showing similarity of *lsrAP*$_2$ to the class III CRP-dependent promoter, in which regulation of *lsrAP*$_2$ may require the interaction of RNA polymerase (RNAP) α subunit C-terminal domains (αCTD) with bound CRP. The locations of the three putative *lsrA* promoters (*lsrAP*$_1$, *lsrAP*$_2$, and *lsrAP*$_3$) are shown along the bottom of the figure, and the putative −10 and −35 sites for each are represented by black boxes. The two *lsrR* promoters (*lsrRP*$_1$ and *lsrRP*$_2$) are shown at the top of the figure, and the putative −10 and −35 sites for each are represented by gray boxes. CRP binding sites are indicated by opposing arrows.

rently not known. However, one possibility is that DNA bending arising from IHF binding to IHFs$_2$ stimulates transcription by effecting a conformational change that alters the structure of the DNA helix and facilitates open complex formation at one or more of the *lsrA* promoters (see below), similar to that described for P_{ilvG} by Parekh and Hatfield (46) or for systems such as phage lambda pL promoter (47) and the *Caulobacter crescentus flbG* promoter (48). 5′-RACE showed that the *lsrA* transcriptional start sites (TSSs) reside a considerable distance upstream from the putative *lsrA* start codon and IHFs$_2$, with the most prominent TSS mapping to nucleotide −210 and two additional sites mapping to nucleotides −184 and −262 at lower frequency. This suggests that *lsrACDBFG* expression may be directed from three promoters, and putative −10 and −35 elements were associated with each of the TSSs identified. Interestingly, elements from each of the putative promoters overlap binding sites for the LsrR repressor, suggesting that a mechanism of LsrR-mediated repression of *lsrACDBFG* may be through restriction of RNA polymerase (RNAP) access to these promoters when LsrR is bound. In addition, the *lsrAP*$_2$ promoter (TSS at −210) is similar to the *lsrA* promoter of *E. coli* (49) and resembles a class III CRP-dependent promoter, possessing two or more CRP binding sites that function to increase binding of RNAP and initiation of transcription (50). Similar to some class III CRP-dependent promoters, *lsrAP*$_2$ contains one CRP site (CRP$_1$) centered approximately 99 nucleotides upstream from the TSS and a second CRP site (CRP$_2$) located around nucleotide −39 and overlapping the −35 element of *lsrAP*$_2$. Indeed, two CRP binding sites located in similar positions in a semisynthetic CRP-dependent promoter resulted in a 2- to 4-fold increase in transcription compared to a semisynthetic promoter with a single CRP site overlapping the −35 element (51). Thus, the two CRP sites in *lsrAP*$_2$ may act cooperatively where one α subunit C-terminal domain (αCTD) of RNAP interacts with the upstream CRP dimer subunit bound at CRP$_2$, the second αCTD interacts with the downstream CRP dimer subunit bound at CRP$_1$, and the downstream subunit of CRP at CRP$_2$ interacts with RNAP α subunit N-terminal domain (αNTD) and σ subunit, consistent with known class III CRP-dependent promoters (Fig. 6).

Or current model is that the regulation of *lsrACDBFG* expression is highly complex and is directed by regulatory elements in a 414-bp region that extends upstream from the ATG codon that is currently annotated as nucleotides +159 to +161 of *lsrA*. Transcription is primarily driven by *lsrAP*$_2$, which produces a transcript containing a 5′-untranslated region of 210 nucleotides. Transcription of the operon may be induced by DNA bending mediated by IHF binding to IHFs$_2$ and by CRP, but it is also negatively controlled by LsrR and an unknown regulatory element in the −1 to −42 region relative to the putative start codon (compare plasmids pATE74 and pATE75 in Fig. 5). Currently it is not known if this additional regulation occurs at the level of transcription or by posttranscriptional mechanisms, such as the activity of small RNAs involved in regulation of polycistronic mRNA (52). Finally, we cannot conclusively exclude the possibility that IHFs$_2$ and other regulatory elements reside within the coding sequence of the gene and that the *lsrA* start codon as currently annotated in the *A. actinomycetemcomitans* genome sequence is correct. Determination of the N-terminal protein sequence of native LsrA would address this possibility.

A second IHF binding site (IHFs$_1$) that interacts with purified IHF complex was located at nucleotides −65 to −77 relative to the *lsrR* start codon. Interestingly, IHF differentially regulates the *lsrRK* and *lsrACDBFG* operons, since a single-copy genomic *lsrRK* promoter-*lacZ* fusion expressed in Δ*ihfA* or Δ*ihfB* backgrounds indicated that IHF negatively regulates *lsrRK* expression. Two TSS were identified by 5′-RACE for the *lsrRK* promoter: the most prevalent TSS mapped to nucleotide −26, and a second site mapped to residue −126 at much lower frequency, and putative −10 and −35 elements were associated with each TSS. Thus, *lsrRK* may be expressed by two promoters. Deletion of *lsrRP*$_1$ (TSS at nucleotide −26) resulted in a significant reduction in *lsrRK* expression, consistent with the RACE results, suggesting that the main TSS occurred at residue −26. In addition, the putative −35 element of *lsrRP*$_1$ overlaps IHFs$_1$, suggesting that downregulation of *lsrRK* by IHF may arise from IHF blocking of RNAP at this promoter. Repression of transcription by IHF binding to sites that overlap core promoter elements has also been described for the *ompB* promoter of *E. coli* (53) and for bacteriophage λ P_L2 and P_R, bacterial *ilvGMEDA* P_G1 and promoters of *ihfA* and *ihfB* genes (54–57). In addition, the downregulation of *lsrRK* by IHF may also indirectly contribute to the induction of *lsrACDBFG* by reducing the levels of the LsrR repressor protein that is produced.

In summary, we have shown that IHF differently regulates the expression of *lsrRK* and *lsrACDBFG* and that each operon may be transcribed by multiple promoters. The essential −10 and/or −35 elements for each of the promoters overlap binding sites for IHF, LsrR, or CRP, suggesting that RNAP competes for binding to the *lsrA* and *lsrR* promoters with these regulatory proteins. Finally, *lsrAP*$_2$ primarily drives expression of *lsrACDBFG*, and this pro-

moter resembles a class III CRP-dependent promoter in which the two CRP binding sites may function cooperatively to stimulate transcription.

ACKNOWLEDGMENT

This research was supported by the Public Health Service grant RO1DE14605 from the NIDCR.

REFERENCES

1. **Aas JA, Paster BJ, Stokes LN, Olsen I, Dewhirst FE.** 2005. Defining the normal bacterial flora of the oral cavity. J. Clin. Microbiol. **43:**5721–5732. http://dx.doi.org/10.1128/JCM.43.11.5721-5732.2005.
2. **Whittaker CJ, Klier CM, Kolenbrander PE.** 1996. Mechanisms of adhesion by oral bacteria. Annu. Rev. Microbiol. **50:**513–552. http://dx.doi.org/10.1146/annurev.micro.50.1.513.
3. **Marsh PD.** 2006. Dental plaque as a biofilm and a microbial community—implications for health and disease. BMC Oral Health **6**(Suppl 1):S14. http://dx.doi.org/10.1186/1472-6831-6-S1-S14.
4. **Marsh PD, Bradshaw DJ.** 1997. Physiological approaches to the control of oral biofilms. Adv. Dent. Res. **11:**176–185. http://dx.doi.org/10.1177/08959374970110010901.
5. **Socransky SS, Haffajee AD.** 1992. The bacterial etiology of destructive periodontal disease: current concepts. J. Periodontol. **63:**322–331. http://dx.doi.org/10.1902/jop.1992.63.4s.322.
6. **Fong KP, Gao L, Demuth DR.** 2003. *luxS* and *arcB* control aerobic growth of *Actinobacillus actinomycetemcomitans* under iron limitation. Infect. Immun. **71:**298–308. http://dx.doi.org/10.1128/IAI.71.1.298-308.2003.
7. **Actis LA, Rhodes ER, Tomaras AP.** 2003. Genetic and molecular characterization of a dental pathogen using genome-wide approaches. Adv. Dent. Res. **17:**95–99. http://dx.doi.org/10.1177/154407370301700122.
8. **James CE, Hasegawa Y, Park Y, Yeung V, Tribble GD, Kuboniwa M, Demuth DR, Lamont RJ.** 2006. LuxS involvement in the regulation of genes coding for hemin and iron acquisition systems in *Porphyromonas gingivalis*. Infect. Immun. **74:**3834–3844. http://dx.doi.org/10.1128/IAI.01768-05.
9. **Kuramitsu HK, He X, Lux R, Anderson MH, Shi W.** 2007. Interspecies interactions within oral microbial communities. Microbiol. Mol. Biol. Rev. **71:**653–670. http://dx.doi.org/10.1128/MMBR.00024-07.
10. **James D, Shao H, Lamont RJ, Demuth DR.** 2006. The *Actinobacillus actinomycetemcomitans* ribose binding protein RbsB interacts with cognate and heterologous autoinducer 2 signals. Infect. Immun. **74:**4021–4029. http://dx.doi.org/10.1128/IAI.01741-05.
11. **Schauder S, Shokat K, Surette MG, Bassler BL.** 2001. The LuxS family of bacterial autoinducers: biosynthesis of a novel quorum-sensing signal molecule. Mol. Microbiol. **41:**463–476. http://dx.doi.org/10.1046/j.1365-2958.2001.02532.x.
12. **Zhao G, Wan W, Mansouri S, Alfaro JF, Bassler BL, Cornell KA, Zhou ZS.** 2003. Chemical synthesis of S-ribosyl-L-homocysteine and activity assay as a LuxS substrate. Bioorg. Med. Chem. Lett. **13:**3897–3900. http://dx.doi.org/10.1016/j.bmcl.2003.09.015.
13. **Block PJ, Yoran C, Fox AC, Kaltman AJ.** 1973. *Actinobacillus actinomycetemcomitans* endocarditis: report of a case and review of the literature. Am. J. Med. Sci. **266:**387–392. http://dx.doi.org/10.1097/00000441-197311000-00006.
14. **Page MI, King EO.** 1966. Infection due to *Actinobacillus actinomycetemcomitans* and *Haemophilus aphrophilus*. N. Engl. J. Med. **275:**181–188. http://dx.doi.org/10.1056/NEJM196607282750403.
15. **Slots J, Reynolds HS, Genco RJ.** 1980. *Actinobacillus actinomycetemcomitans* in human periodontal disease: a cross-sectional microbiological investigation. Infect. Immun. **29:**1013–1020.
16. **Zambon JJ, DeLuca C, Slots J, Genco RJ.** 1983. Studies of leukotoxin from *Actinobacillus actinomycetemcomitans* using the promyelocytic HL-60 cell line. Infect. Immun. **40:**205–212.
17. **Marsh PD.** 2003. Are dental diseases examples of ecological catastrophes? Microbiology **149:**279–294. http://dx.doi.org/10.1099/mic.0.26082-0.
18. **Novak EA, Shao H, Daep CA, Demuth DR.** 2010. Autoinducer-2 and QseC control biofilm formation and in vivo virulence of *Aggregatibacter actinomycetemcomitans*. Infect. Immun. **78:**2919–2926. http://dx.doi.org/10.1128/IAI.01376-09.
19. **Schaeffer LM, Schmidt ML, Demuth DR.** 2008. Induction of *Aggregatibacter actinomycetemcomitans* leukotoxin expression by IS*1301* and *orfA*. Microbiology **154:**528–538. http://dx.doi.org/10.1099/mic.0.2007/012195-0.
20. **Shao H, Lamont RJ, Demuth DR.** 2007. Autoinducer 2 is required for biofilm growth of *Aggregatibacter* (*Actinobacillus*) *actinomycetemcomitans*. Infect. Immun. **75:**4211–4218. http://dx.doi.org/10.1128/IAI.00402-07.
21. **McNab R, Lamont RJ.** 2003. Microbial dinner-party conversations: the role of LuxS in interspecies communication. J. Med. Microbiol. **52:**541–545. http://dx.doi.org/10.1099/jmm.0.05128-0.
22. **Shao H, James D, Lamont RJ, Demuth DR.** 2007. Differential interaction of *Aggregatibacter* (*Actinobacillus*) *actinomycetemcomitans* LsrB and RbsB proteins with autoinducer 2. J. Bacteriol. **189:**5559–5565. http://dx.doi.org/10.1128/JB.00387-07.
23. **Diaz Z, Xavier KB, Miller T.** 2009. The crystal structure of the *Escherichia coli* autoinducer-2 processing protein LsrF. PLoS One **28:**e6820. http://dx.doi.org/10.1371/journal.pone.0006820.
24. **Marques JC, Lamosa P, Russell C, Ventura R, Maycock C, Semmelhack MF, Miller ST, Xavier KB.** 2011. Processing the interspecies quorum-sensing signal autoinducer-2 (AI-2): characterization of phospho-(S)-4,5-dihydroxy-2,3-pentanedione isomerization by LsrG protein. J. Biol. Chem. **286:**18331–18343. http://dx.doi.org/10.1074/jbc.M111.230227.
25. **Taga ME, Miller ST, Bassler BL.** 2003. Lsr-mediated transport and processing of AI-2 in *Salmonella* Typhimurium. Mol. Microbiol. **50:**1411–1427. http://dx.doi.org/10.1046/j.1365-2958.2003.03781.x.
26. **Xavier KB, Bassler BL.** 2005. Regulation of uptake and processing of the quorum-sensing autoinducer AI-2 *in Escherichia coli*. J. Bacteriol. **187:**238–248. http://dx.doi.org/10.1128/JB.187.1.238-248.2005.
27. **Torres-Escobar A, Juárez-Rodríguez MD, Lamont RJ, Demuth DR.** 2013. Transcriptional regulation of *Aggregatibacter actinomycetemcomitans lsrACDBFG* and *lsrRK* operons and their role in biofilm formation. J. Bacteriol. **195:**56–65. http://dx.doi.org/10.1128/JB.01476-12.
28. **Craig N, Nash HA.** 1984. *E. coli* integration host factor binds to specific sites in DNA. Cell **39:**707–716. http://dx.doi.org/10.1016/0092-8674(84)90478-1.
29. **Friedman DI** 1988. Integration host factor: a protein for all reasons. Cell **55:**545–554. http://dx.doi.org/10.1016/0092-8674(88)90213-9.
30. **Goodrich JA, Schwartz ML, McClure WR.** 1990. Searching for and predicting the activity of sites for DNA binding proteins: compilation and analysis of the binding sites for *Escherichia coli* integration host factor (IHF). Nucleic Acid Res. **18:**4993–5000. http://dx.doi.org/10.1093/nar/18.17.4993.
31. **van Rijn PA, van de Putte P, Goosen N.** 1991. Analysis of the IHF binding site in the regulatory region of bacteriophage Mu. Nucleic Acid Res. **19:**2825–2834. http://dx.doi.org/10.1093/nar/19.11.2825.
32. **Nash HA.** 1981. Integration and excision of bacteriophage lambda: the mechanism of conservation site specific recombination. Annu. Rev. Genet. **15:**143–167. http://dx.doi.org/10.1146/annurev.ge.15.120181.001043.
33. **Mangan MW, Lucchini S, Danino V, Cróinín TO, Hilton JC, Dorman CJ.** 2006. The integration host factor (IHF) integrates stationary-phase and virulence gene expression in *Salmonella enterica* serovar Typhimurium. Mol. Microbiol. **59:**1831–1847. http://dx.doi.org/10.1111/j.1365-2958.2006.05062.x.
34. **Yona-Nadler C, Umanski T, Aizawa S, Friedberg D, Rosenshine I.** 2003 Integration host factor (IHF) mediates repression of flagella in enteropathogenic and enterohaemorrhagic *Escherichia coli*. Microbiology **149:**877–884. http://dx.doi.org/10.1099/mic.0.25970-0.
35. **Marques MV, Gober JW.** 1995. Activation of a temporally regulated *Caulobacter* promoter by upstream and downstream sequence elements. Mol. Microbiol. **16:**279–289. http://dx.doi.org/10.1111/j.1365-2958.1995.tb02300.x.
36. **Beach MB, Osuna R.** 1998. Identification and characterization of the *fis* operon in enteric bacteria. J. Bacteriol. **180:**5932–5946.
37. **Goshima N, Kano Y, Tanaka H, Kohno K, Iwaki T, Imamoto F.** 1994. IHF suppresses the inhibitory effect of H-NS on HU function in the *hin* inversion system. Gene **141:**17–23. http://dx.doi.org/10.1016/0378-1119(94)90122-8.
38. **Blomfield IC, Kulasekara DH, Eisenstein BI.** 1997. Integration host factor stimulates both FimB- and FimE-mediated site-specific DNA inversion that controls phase variation of the type 1 fimbria expression in *Escherichia coli*. Mol. Microbiol. **23:**705–717. http://dx.doi.org/10.1046/j.1365-2958.1997.2241615.x.
39. **Goodman SD, Obergfell KP, Jurcisek JA, Downey JS, Ayala EA, Tjokro N, Li B, Justice SS, Bakaletz LO.** 2011. Biofilms can be dispersed by

focusing the immune system on a common family of bacterial nucleoid-associated proteins. Mucosal Immunol. **4:**625–637. http://dx.doi.org/10.1038/mi.2011.27.
40. **Brandstetter KA, Jurcisek JA, Goodman SD, Bakaletz LO, Das S.** 2013. Antibodies directed against integration host factor mediated biofilm clearance from Nanospore. Laryngoscope **123:**2626–2632. http://dx.doi.org/10.1002/lary.24183.
41. **Gustave JE, Jurcisek JA, McCoy KS, Goodman SD, Bakaletz LO.** 2013. Targeting bacterial integration host factor to disrupt biofilms associated with cystic fibrosis. J. Cyst. Fibros. **12:**384–389. http://dx.doi.org/10.1016/j.jcf.2012.10.011.
42. **Sambrook J, Russell DW.** 2001. Molecular cloning: a laboratory manual, 3rd ed. Cold Spring Harbor Laboratory Press, Cold Spring Harbor, NY.
43. **Juárez-Rodríguez MD, Torres-Escobar A, Demuth DR.** 2013. Construction of new cloning, *lacZ* reporter and scarless-markerless suicide vectors for genetic studies in *Aggregatibacter actinomycetemcomitans*. Plasmid **69:**211–222. http://dx.doi.org/10.1016/j.plasmid.2013.01.002.
44. **Torres-Escobar A, Juárez-Rodríguez MD, Curtiss R.** 2010. Biogenesis of *Yersinia pestis* PsaA in recombinant attenuated *Salmonella* Typhimurium vaccine (RASV) strain. FEMS Microbiol. Lett. **302:**106–113. http://dx.doi.org/10.1111/j.1574-6968.2009.01827.x.
45. **Miller JH.** 1972. Experiments in molecular genetics. Cold Spring Harbor Laboratory, Cold Spring Harbor, NY.
46. **Parekh BS, Hatfield GW.** 1996. Transcriptional activation by protein-induced DNA bending: evidence for a DNA structural transmission model. Proc. Natl. Acad. Sci. U. S. A. **93:**1173–1177. http://dx.doi.org/10.1073/pnas.93.3.1173.
47. **Giladi H, Gottesman M, Oppenheim AB.** 1990. Integration host factor stimulates the phage lambda pL promoter. J. Mol. Biol. **213:**109–121. http://dx.doi.org/10.1016/S0022-2836(05)80124-X.
48. **Gober JW, Shapiro L.** 1990. Integration host factor is required for the activation of developmentally regulated genes in *Caulobacter*. Genes Dev. **4:**1494–1504. http://dx.doi.org/10.1101/gad.4.9.1494.
49. **Byrd CM.** 2011. Local and global gene regulation analysis of the autoinducer-2 mediated quorum sensing mechanism in *Escherichia coli*. Ph.D. thesis. University of Maryland, College Park, MD.
50. **Busby S, Ebright RH** 1999. Transcription activation by catabolite activator protein (CAP). J. Mol. Biol. **293:**199–213. http://dx.doi.org/10.1006/jmbi.1999.3161.
51. **Belyaeva TA, Rhodius VA, Webster CL, Busby SJ.** 1998. Transcription activation at promoters carrying tandem DNA sites for the Escherichia coli cyclic AMP receptor protein: organisation of the RNA polymerase alpha subunits. J. Mol. Biol. **277:**789–804. http://dx.doi.org/10.1006/jmbi.1998.1666.
52. **Rice JB, Balasubramanian D, Vanderpool CK.** 2012. RNA binding-site multiplicity involved in translational regulation of a polycistronic mRNA. Proc. Natl. Acad. Sci. U. S. A. 109:E2691–E2698. http://dx.doi.org/10.1073/pnas.1207927109.
53. **Tsui P, Huang L, Freundlich M.** 1991. Integration host factor binds specifically to multiple sites in the *ompB* promoter of *Escherichia coli* and inhibits transcription. J. Bacteriol. **173:**5800–5807.
54. **Giladi H, Murakami K, Ishihama A, Oppenheim AB.** 1996. Identification of an UP element within the IHF binding site at the PL1-PL2 tandem promoter of bacteriophage λ. J. Mol. Biol. **260:**484–491. http://dx.doi.org/10.1006/jmbi.1996.0416.
55. **Kur J, Hasan N, Szybalski W.** 1989. Physical and biological consequences of interactions between integration host factor (IHF) and coliphage lambda late P′R promoter and its mutants. Gene **81:**1–15. http://dx.doi.org/10.1016/0378-1119(89)90331-4.
56. **Tsui P, Freundlich M.** 1988. Integration host factor binds specifically to sites in the *ilvGMEDA* operon in Escherichia coli. J. Mol. Biol. **203:**817–820. http://dx.doi.org/10.1016/0022-2836(88)90212-4.
57. **Aviv M, Giladi H, Schreiber G, Oppenheim AB, Glaser G.** 1994. Expression of the genes coding for the *Escherichia coli* integration host factor are controlled by growth phase, *rpoS*, ppGpp and by autoregulation. Mol. Microbiol. **14:**1021–1031. http://dx.doi.org/10.1111/j.1365-2958.1994.tb01336.x.
58. **Kolenbrander PE, London J.** 1993. Adhere today, here tomorrow: oral bacterial adherence. J. Bacteriol. **175:**3247–3252.
59. **Lamont RJ, Jenkinson HF.** 1998. Life below the gum line: pathogenic mechanisms of *Porphyromonas gingivalis*. Microbiol. Mol. Biol. Rev. **62:**1244–1263.
60. **Paster BJ, Olsen I, Aas JA, Dewhirst FE.** 2006. The breadth of bacterial diversity in the human periodontal pocket and other oral sites. Periodontol. 2000 **42:**80–87. http://dx.doi.org/10.1111/j.1600-0757.2006.00174.x.